ACS OMEGA

Open Access

http://pubs.acs.org/journal/acsodf

Article

Study on Gas−Liquid Coaxial Jet Foam Generator and Its Foaming Characteristics

Caiyuan Lu, Xiaoxing Zhong,* Mujun Chen, and Yuntao Liang

Cite This: *ACS Omega* 2024, 9, 31646−31656

Read Online

ACCESS | Metrics & More | Article Recommendations

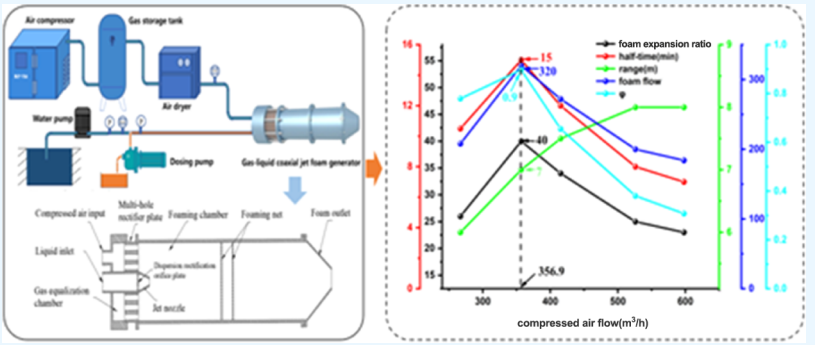

ABSTRACT: In order to solve the difficulty of the existing compressed air foam system with low FER and difficult in having both the FER and range. A new type of foam generator for CAFS was designed, an air−liquid coaxial foam generator, which produces foam with high FER (the ratio of the foam volume to the volume of the foam solution) and large output momentum. In this paper, experiments on the foam production performance of a gas−liquid coaxial jet foam generator were carried out with different parameters, such as liquid flow rate, gas flow rate, and foam output end diameter. The variation of FER, foam half-life, range, foam volume, and compressed air utilization rate with the experimental parameters were analyzed. The results show that the foaming performance of the foam generator tends to rise in the range of 8−12.4 m^3/h at a fixed gas flow rate, the FER and foam half-life are negatively related to it, and the foaming performance tends to decrease in the range of 12.4−18 m^3/h. The best foaming performance was achieved when the liquid volume of the foam generator was 12.4 m^3/h. For the liquid volume value in different intervals, the foaming performance varies with the air supply volume. When the liquid volume is higher than 12.4 m^3/h, increasing the air supply volume is beneficial to improve the foaming performance, and when the liquid volume is lower than 12.4 m^3/h, increasing the air volume does not improve the foaming performance. The effect of the diameter of the foaming chamber on the foaming performance is not monotonic, and an optimum value exists. Compared with similar devices, the gas−liquid coaxial jet foam generator has strong advantages in FER and range and has better application prospects for fire control in restricted spaces.

1. INTRODUCTION

With the rapid development of social and economic development, the industrialization and urbanization process continues to accelerate. In particular, high-rise buildings, underground projects, flammable and explosive units, and high-density, large space of public gathering places continue to emerge. The fire-fighting operations and emergency rescue involving the breadth, complexity, and disposal difficulties are increasing.[1] In 2021, there were 745,000 fires in China, with direct property losses of 6.75 billion ¥, causing huge losses to national and people's lives and property.[2] The disadvantages of traditional fire-fighting technology in the field as the first emergency rescue force are gradually emerging,[3] while compressed air foam systems (CAFS) are gradually being promoted and developed as an energy-saving, environmentally friendly and efficient fire-fighting technology.[4] CAFS has the advantages of high foam momentum, high fire-extinguishing efficiency, long retention time, easy adjustment of the FER, and lightweight of the water belt, which is of common interest worldwide.

The foam generator is the key part in CAFS to make foam liquid and compressed air mix with each other to generate foam. Scholars have also carried out a lot of research. Jiaqing et al.[5] set the water and high-pressure gas flow ports vertically to enhance the foam generator mixing and foaming effect. Jia[6]

Received: February 28, 2024
Revised: May 26, 2024
Accepted: June 28, 2024
Published: July 10, 2024

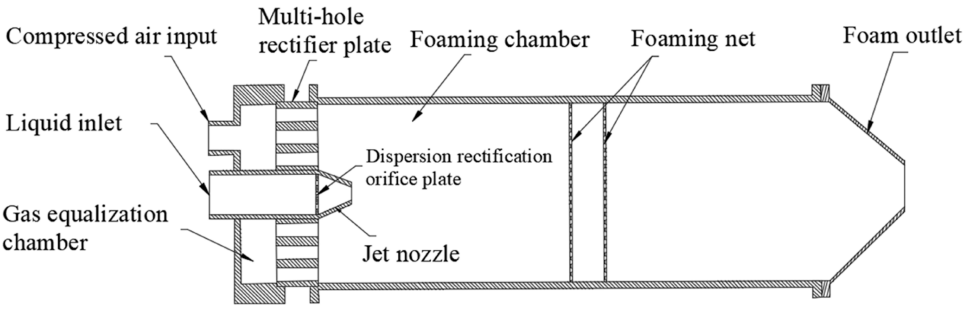

Figure 1. Structure of the gas−liquid coaxial jet foam generator.

provided a gas−liquid mixing device in which a compressed air line is inserted vertically into a mixing liquid tube with uniform inlet round holes around the air tube. The air and liquid flows are opposed to each other, increasing the contact area between the air and the mixing fluid. Jie et al.[7] inserted the gas line into the liquid inlet line and arranged the gas dispersal pipe in the opposite direction to the liquid flow, and the end of the gas dispersal pipe was connected to the bulkhead. In this way, the gas−liquid mixing effect is enhanced. Cheng et al.[8] used a divider to evenly separate the mixing channels, and the inlet pipe was set in the gas−liquid mixing pipe. The foam mixture enters the foaming line through the mixing channel, and a number of uniformly spaced foaming nets are installed inside the foaming line. Ye[9] studied the foaming effect of T-mixers with built-in baffles. It was found that the FER increased and then decreased as the inlet pressure increased. At the optimum operating condition, the inlet pressure was 0.65 MPa, and the FER was 24.7. Xinixao[10] designed a spiral jet-type foam generator. It was found that the FER rose and then fell with the increase of the liquid flow. At a flow rate of 4 m^3/h, the maximum FER value of 94 was reached, but the range was less than 1 m. Jushi[11,12] et al. designed a foam generator by combining a T-shaped air inlet with net foaming. When the liquid flow rate was 18 L/min and the gas flow rate was 30 m^3/h, the foam flow rate reached a maximum value of 515 L/min, and the FER was 22. Lei[13] et al. designed a composite foam generator with a combination of filled glass beads and porous orifice plates with an FER of 31.6. However, the device has a large local loss in the filling space and requires a high inlet pressure. Youying et al.[14] designed a net foaming apparatus with a foaming net diameter of 2 mm, five layers of foaming net, a foaming net thickness of 2 mm, and a foaming net spacing of 7 cm. The optimum gas−liquid ratio was 55, the maximum FER was 53.57, and the maximum foam injection distance was 6 m. Qin[15] et al. designed a three-phase foam generator for mining, using a combination of venturi, collector, and impeller for foaming. The foam produced was uniform and fine, but the FER was low. Minwen et al.[16] provided a concentric tube-type foam generator to prepare homogeneous foam, but the structure is complex and requires high water quality. Stec et al.[17] analyzed the mixing homogeneity of two types of static mixers and the pressure and aspect ratio parameters had an effect on the homogeneity of the above mixers. Brian et al.[18−20] designed a mesh foaming apparatus for laboratory use that produced high-frequency foam but with low outlet momentum. Liu et al.[21,22] found, in a simulation study, that the spiral baffle-type foam generator has a uniform gas−liquid mixture and better foaming effect at a gas−liquid ratio of 30 to 40%.

At present, CAFS is generally not equipped with a special gas−liquid mixer,[23] and the mixture of compressed air and foam is mostly stirred and mixed in the pipeline to generate fire-extinguishing foam. Furthermore, existing foam generators have the disadvantage of high FER and high foam outlet momentum, which are difficult to have both. In order to solve the above shortcomings, this paper independently designed a new gas−liquid coaxial jet foam generator device for CAFS. Foaming experiments with different outlet structures and gas-to-liquid ratios were carried out to analyze the foaming characteristics of the foam-generating units and to obtain the optimum operating parameters. Experiments with different foam-generating units were also carried out to compare the foaming performance of the foam-generating units.

2. CONSTRUCTION DESIGN OF FOAM GENERATOR

2.1. Foam Generator Construction. The basic structure of the gas−liquid coaxial jet foam generator is shown in Figure 1. It is mainly composed of the compressed air inlet, liquid inlet, gas equalization chamber, porous rectification orifice tray, multihole rectifier plate, jet nozzle, foaming chamber, and foaming net. The dimensions of the system components are as follows: the compressed air inlet has a diameter of 30 mm, the liquid inlet has a diameter of 50 mm, the foaming chamber has a diameter of 220 mm and a length of 600 mm, the jet nozzle has a diameter of 16 mm, and the foaming net is located in the middle of the foaming chamber with a mesh size of 20. The design of the device has the following advantages.

(1) Instead of the traditional T-shaped gas−liquid piping design, the device uses axial water−gas two-phase and axial two-phase gas−liquid inlet power to fully mix, resulting in enhanced foam generator performance and foam kinetic energy export, while significantly reducing resistance losses.

(2) The device uses a multihole rectifier plate to ensure uniform air intake, preventing poor foaming and low-foam stability caused by large gaps between gas velocity and flow rate, thereby improving foaming efficiency. In contrast, traditional intake pipelines lack this structure, resulting in uneven air intake.

(3) The device adopts a net-type jet composite foaming structure. According to the theory of turbulent jet boundary layer, the liquid phase jet starts diffusing in a cone shape from inside to outside in the direction of the nozzle outlet axis. To improve the utilization rate of the foam solution, the degree of mixing between the foam solution and air is improved, and the foaming effect is enhanced. The traditional use of spiral jet foam structure spray foam solution, resistance is too large and uneven,

https://doi.org/10.1021/acsomega.4c01862
ACS Omega 2024, 9, 31646−31656

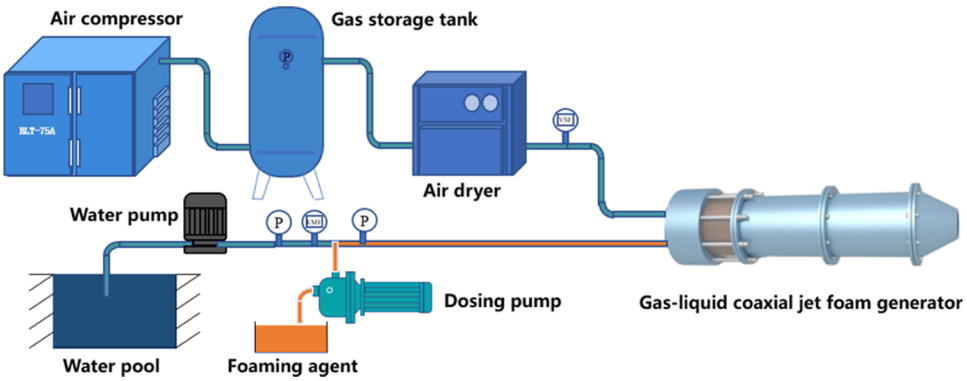

Figure 2. Experimental system.

resulting in low FER, small export momentum, and low range.

2.2. Mechanism of Foam Generation. Compressed air passes through the multihole rectifier plate to make the overall flow uniform in the cross section and then reaches the foaming chamber. The foam mixture improves dispersion after passing through the dispersion rectification orifice plate and moves rapidly outward in a conical shape at the nozzle. This increases the contact area with the air and creates a negative pressure roll in the jet ring area to suck the compressed air entering the foaming chamber. As the injection distance increases, the compressed air and foam mixture are continuously mixed due to the viscosity and velocity difference between the jet boundary layer and the gas. As a result, the outer interface of the jet presents a certain velocity gradient distribution, forming an outward scattering flow state. First, the foam mixture reaches the foaming net and is fully covered, and the gas passes through the mesh to carry out the foaming process. Then, the hydrophobic groups in the blowing agent face the gas phase, and the hydrophilic groups face the liquid phase and are closely arranged to form a large number of foam populations with a two-phase medium. Finally, the gas is continuously blown and sheared to form foam, which is rectified and sprayed out through the port of the foaming chamber.

3. EXPERIMENTS

3.1. Experiment System. The experimental system is shown in Figure 2, mainly consisting of an air compressor, a water pump, a dosing pump, a vortex flow meter, an electromagnetic flow meter, and a gas−liquid coaxial jet foam generator. The air compressor (BLT-75A) can adjust the air volume range of 0−600 m^3/h and the pressure of 0−0.8 MPa. The pump pressure is 0−0.8 MPa and the flow rate is 0−18 m^3/h. The dosing pump is used to add foam liquid, and the flow rate is 0−1.2 m^3/h. Table 1 is the specification of the main test instrument.

3.2. Experimental Materials and Parameters. The foaming agent used in the experiment was a commonly used general-purpose extinguishing agent on the market, and the foam liquid was added at a ratio of 3%. In order to ensure the accuracy of the experimental adjustment of the gas−liquid ratio, the gas flow rate of the air compressor was experimentally measured, as shown in Figure 3. When the pressure of the air compressor is 0.1−0.3 MPa, the gas flow is linearly related to the air pressure. After the pressure of the air compressor reaches 0.3 MPa, the gas flow is 597.901 m^3/h, and

Table 1. Specification of the Main Test Instrument

instrument name	measuring range	precision	manufacturer
Gas vortex flow meter	0−4800 m^3/h	1.0%	Jiangsu Aikete Instrument Factory
electromagnetic flow meter(YL-LDE-65)	4−120 m^3/h	0.5%	Jiangsu Yalong Measurement and Control Group Co., Ltd.
water pump pressure gauge P_1	0−16 MPa	0.5%	Jiangsu Yalong Measurement and Control Group Co., Ltd.
inlet pressure gauge P_2	0−6 MPa	0.5%	Shanghai Yimin Instrument Co., Ltd.
measuring bucket	0−20 L	0.1 L	Hebei Guanzhuo Testing Technology Co., Ltd.
ruler	0−30 m	0.002 m	Ningbo Deli Tools Co., Ltd.
electronic balance	100−10,000 g	0.5%	Yongkang Wuxin Weighing Apparatus Co., Ltd.

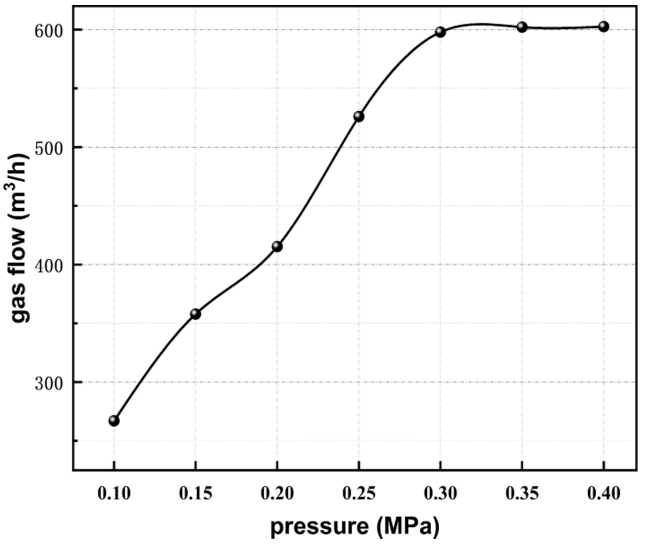

Figure 3. Curve of change of air volume with air pressure.

then, the gas flow remains stable. In this paper, the experimental gas flow is controlled by adjusting the air pressure of the air compressor, and the water flow is controlled by a butterfly valve installed in the water pipeline.

The foaming performance of gas−liquid coaxial jet foam generator includes the FER, foam volume, foam half-life, range, and utilization rate of pressure gas, as defined below.

(1) The FER is the ratio of the foam volume to the volume of the foam solution, which is measured and calculated

https://doi.org/10.1021/acsomega.4c01862
ACS Omega 2024, 9, 31646−31656

by the weighing method[24] in this paper. The formula is as follows

$$\mathrm{FER} = \rho V/(W_1 - W_2) \quad (1)$$

where V is the foam volume, L; W_1 is the weight of the measuring barrel after containing the liquid, W_2 is the weight of the measuring barrel, kg; and ρ is the density of the foam mixture, calculated as 1 kg/L.

(2) The foam flow (Q) is the flow of the foam generated by the foam generator. In this paper, the product of the FER and the water flow rate are used. The calculation formula is as follows

$$Q = FER \times q \quad (2)$$

(3) Half-life, the time required for 50% of its mass to separate from the foam when the foam liquid is drained.[25] The shorter the bubble half-life, the faster the foam bursts.

$$\text{Half life} = t_{m/2} \quad (3)$$

(4) Range is the distance measured from the outlet of the foam generator to the point where the foam stream reaches the ground.

(5) The utilization rate of compressed air is defined as the ratio of the amount of foam generated to the volume flow rate of compressed air.

$$\varphi = Q/Q_{\mathrm{air}} \quad (4)$$

where Q_{air} is the volume of compressed air.

3.3. Experiment Procedure. First, connect the gas−liquid coaxial jet foam generator to the liquid inlet pipeline and check the pipeline to ensure that the joints are firmly connected and tightly sealed. Place the suction pipe of the dosing pump below the liquid level of the prefabricated foam mixture. Preset the air compressor pressure. Then, start the air compressor and use the vortex flow meter to measure the gas flow. Wait for the flow rate to stabilize and then turn on the pump, use the manual control valve to adjust the flow rate, and observe the electromagnetic flow meter. After the flow rate has stabilized, turn on the dosing pump to add foam liquid and observe the foam production effect of the gas−liquid coaxial jet foam generator. Finally, the dosing pump, foam pump, and air compressor were switched off in turn at the end of the experiment. During the experiment, the range of the foam was measured using a ruler. A measuring bucket was used to collect the foam produced by the air−liquid coaxial jet foam-generating unit. Using an electronic balance scale, the FER and foam half-life were calculated and recorded. These steps were repeated for the other groups of experiments.

4. RESULTS AND DISCUSSION

4.1. Effect of Liquid Flow on Foaming Performance. The independent factors affecting the foaming performance of the gas−liquid coaxial jet foam generator are selected, including liquid flow rate, gas flow rate, and outlet diameter. In order to study the influence of each parameter on the foaming performance, this paper explores each factor separately. Figure 4 shows the foam production performance of the gas−liquid coaxial jet foam generator changes with the liquid flow. The gas flow rate is 597 m^3/h, and the liquid flow rate is 8, 10, 12.4, 15, and 18 m^3/h, respectively.

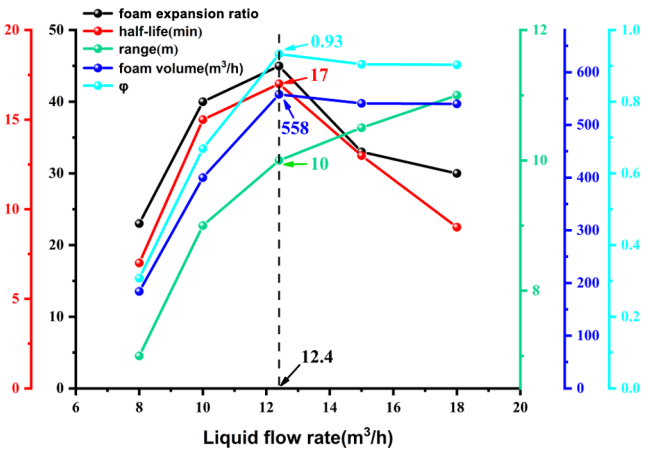

Figure 4. Foaming performance parameters change with liquid flow.

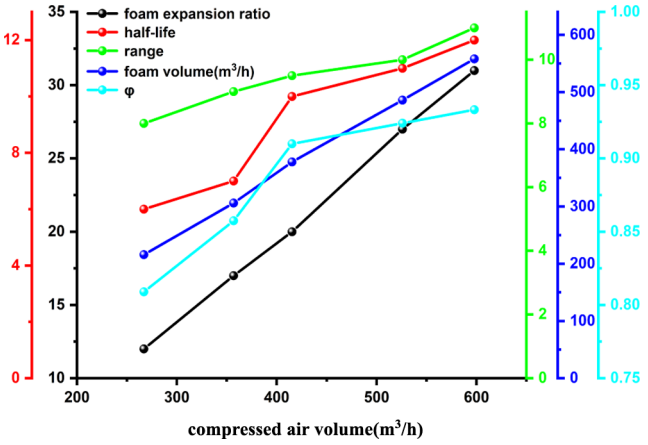

Figure 5. Variation of foaming performance parameters with gas volume (liquid flow 18 m^3/h).

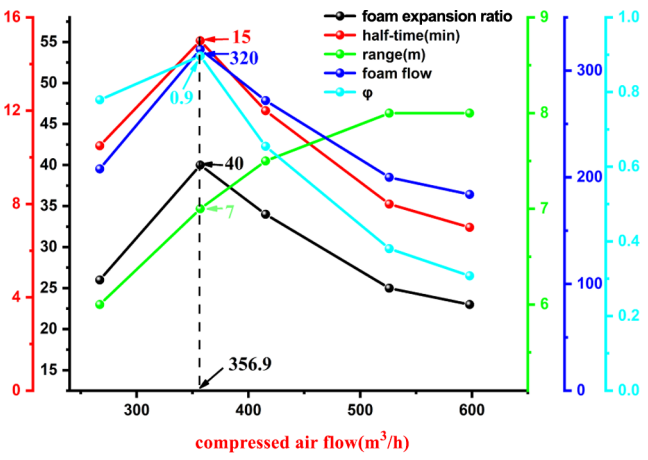

Figure 6. Variation of foaming performance parameters with gas volume (liquid flow 12.4 m^3/h).

The amount of foam Q and the utilization rate of compressed air φ showed a trend of increasing first and then remaining stable with the increase of the liquid flow rate. The turning point is at the liquid flow rate of 12.4 m^3/h. At this time, increasing the liquid flow will not continue to increase the amount of foam and the utilization rate of compressed air. Compared with the liquid flow of 18 m^3/h and the liquid flow of 12.4 m^3/h, the amount of foam and the utilization rate of

https://doi.org/10.1021/acsomega.4c01862
ACS Omega 2024, 9, 31646−31656

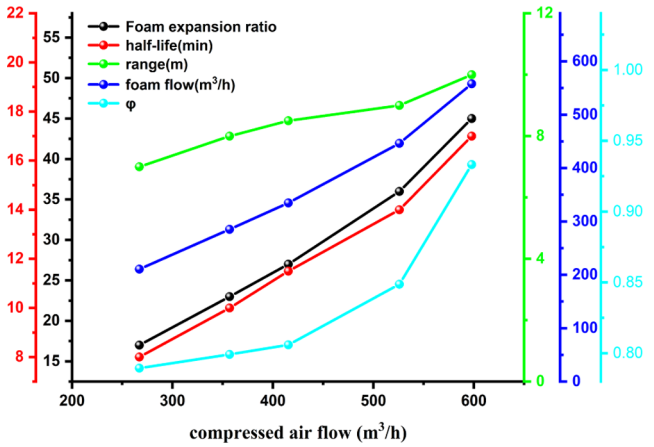

Figure 7. Variation of foaming performance parameters with gas volume (liquid flow 8 m^3/h).

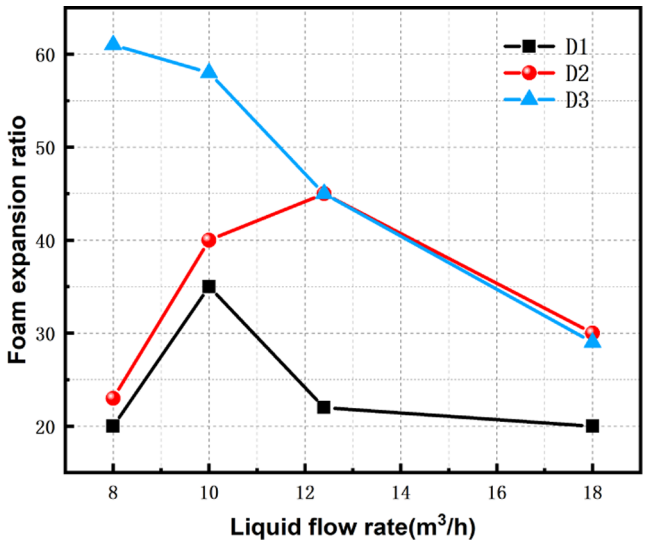

Figure 8. FER changes with the liquid volume under different outlet diameters.

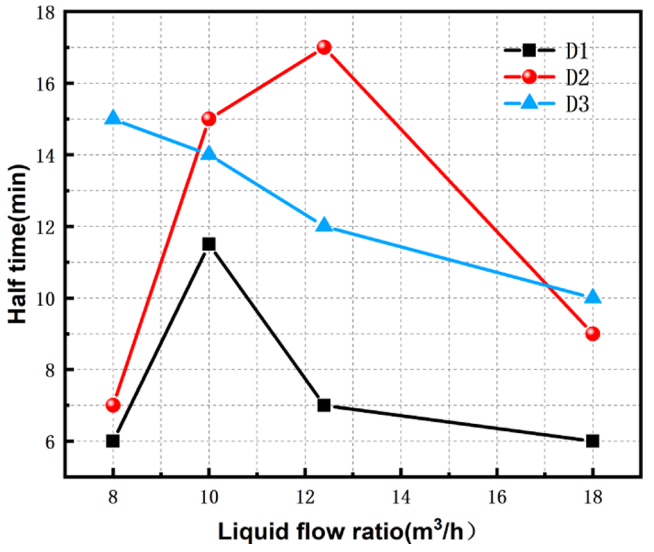

Figure 9. Half-life varies with the liquid volume under different outlet diameters.

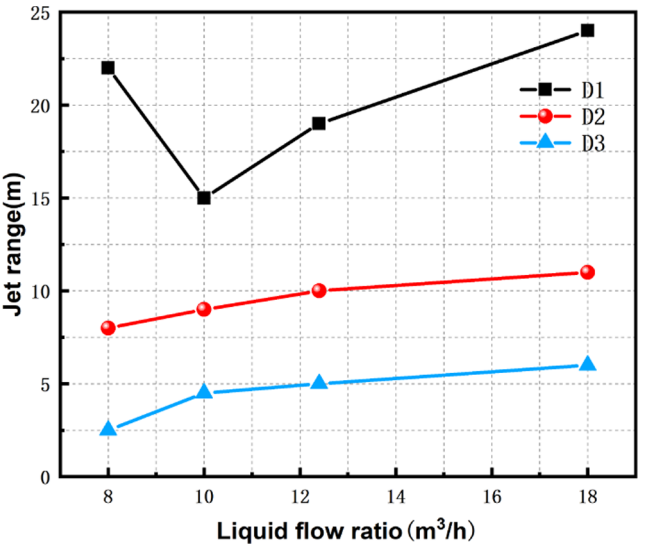

Figure 10. Variation of jet range with liquid volume at different outlet diameters.

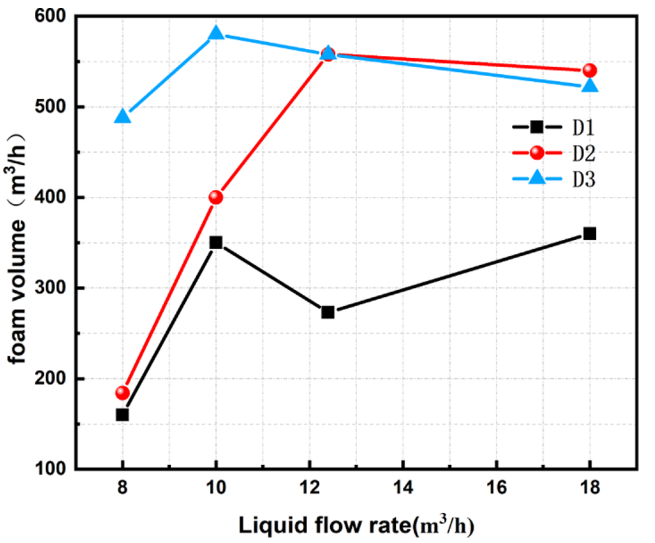

Figure 11. Variation of foam volume with liquid volume at different outlet diameters.

compressed air decreased by about 3.2%. Because the latter compressed air and the foam mixture are fully foamed in the foam cavity, and form foam streams to be ejected. Foam is a multiphase dispersion system, which is the result of the dispersion of the gas phase in the liquid phase. The formation of foam must achieve two conditions: (1) the contact between the gas phase and the liquid phase. This is because the foam is dispersed in the liquid phase of the gas phase in the formation of a multiphase system, so only full contact between the gas phase and the liquid phase will produce foam; this is the liquid phase of the formation of foam necessary and not sufficient conditions and (2) the liquid phase of the bubble faster than the rate of bubble bursting. Since our foam generator foams dynamically, we are able to satisfy condition (2), whereas when the liquid flow rate is certain, there is no excess liquid for gas−liquid combination after the gas is sufficiently supplied, which does not satisfy condition (1), leading to the above law.

The range of the foam jet increases gradually with the increase of the liquid volume. When the liquid volume is 8 $m^3/$

https://doi.org/10.1021/acsomega.4c01862
ACS Omega 2024, 9, 31646−31656

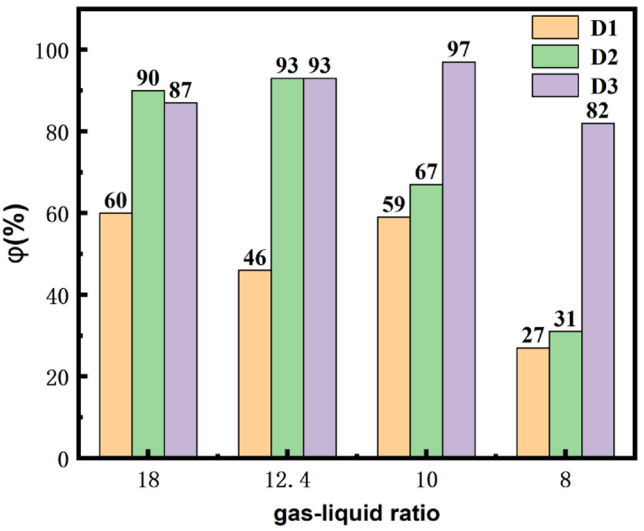

Figure 12. Utilization rate of compressed air varies with liquid volume under different outlet diameters.

Table 2. Experimental Data of Gas-Liquid Coaxial Foam Generator

compressed air pressure (MPa)	liquid flow (m^3/h)	air volume flow (m^3/h)	gas-to-liquid ratio	FER	range (m)	foam volume flow (m^3/h)
0.3	18	597.9	33	30	11	540
0.3	12.4	597.9	48	45	10	558
0.3	10	597.9	60	40	9	400
0.3	8	597.9	75	23	8	184

Table 3. Experimental Data of the Venturi Foam Generator

compressed air pressure (MPa)	liquid flow (m^3/h)	air volume flow (m^3/h)	gas-to-liquid ratio	FER	range (m)	foam volume flow (m^3/h)
0.3	18	597.9	33	23	6	414
0.3	12.4	597.9	48	30	5	372
0.3	10	597.9	60	28	5.5	280
0.3	8	597.9	75			

Table 4. Experimental Data of Spiral Jet-Type Foam Generator

compressed air pressure (MPa)	liquid flow (m^3/h)	air volume flow (m^3/h)	gas-to-liquid ratio	FER	range (m)
0.055	2	384.2	192.1	83.6	<1
0.084	3	311.9	103.9	94.2	<1
0.103	4.5	251.9	56.0	90.4	<1
0.129	5.0	239.5	47.9	74.1	<1

h, the range is 7 m, and when the liquid volume is 18 m^3/h, the range reaches 11 m. Due to the low liquid flow, the gas flow rate is large when the liquid volume is 8 m^3/h and the gas–liquid ratio is 75. The two conditions for foaming are met. However, excessive gas dynamics disrupt the balance of forces within the foam. After the foaming agent is foamed, it is easy to break under the continuous action of the compressed air, and the foam is easy to appear the phenomenon of atomization. At the same time, the amount of foam produced is small, the foaming cavity is not completely filled, and the distribution of

Figure 13. Foaming effect of gas–liquid coaxial and Venturi tube foam generator (photograph courtesy of author).

Table 5. Model Mesh Quality

mesh count	nodes	average mesh quality	maximum aspect ratio	minimum orthogonal quality
114,063	630,019	0.7977	6.58821	0.202235

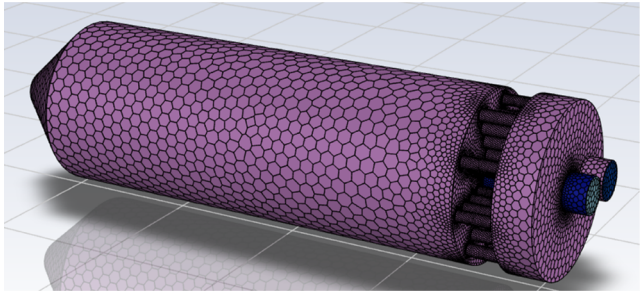

Figure 14. Three-dimensional mesh generation of coaxial jet foam generator.

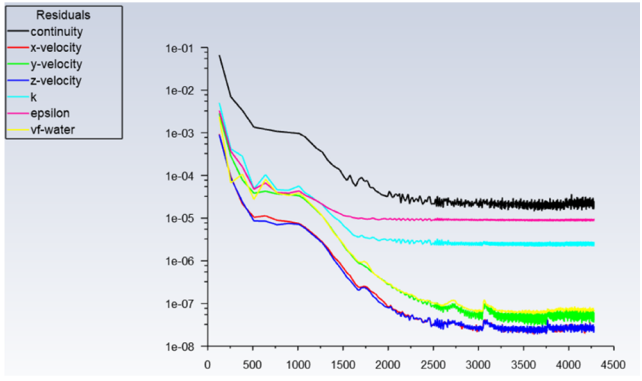

Figure 15. Fluent residual diagram of numerical simulation.

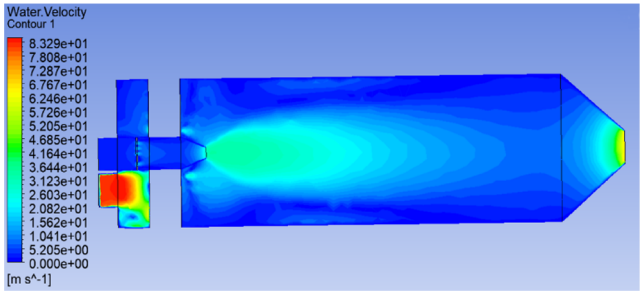

Figure 16. Cloud diagram of liquid phase velocity distribution.

https://doi.org/10.1021/acsomega.4c01862
ACS Omega 2024, 9, 31646–31656

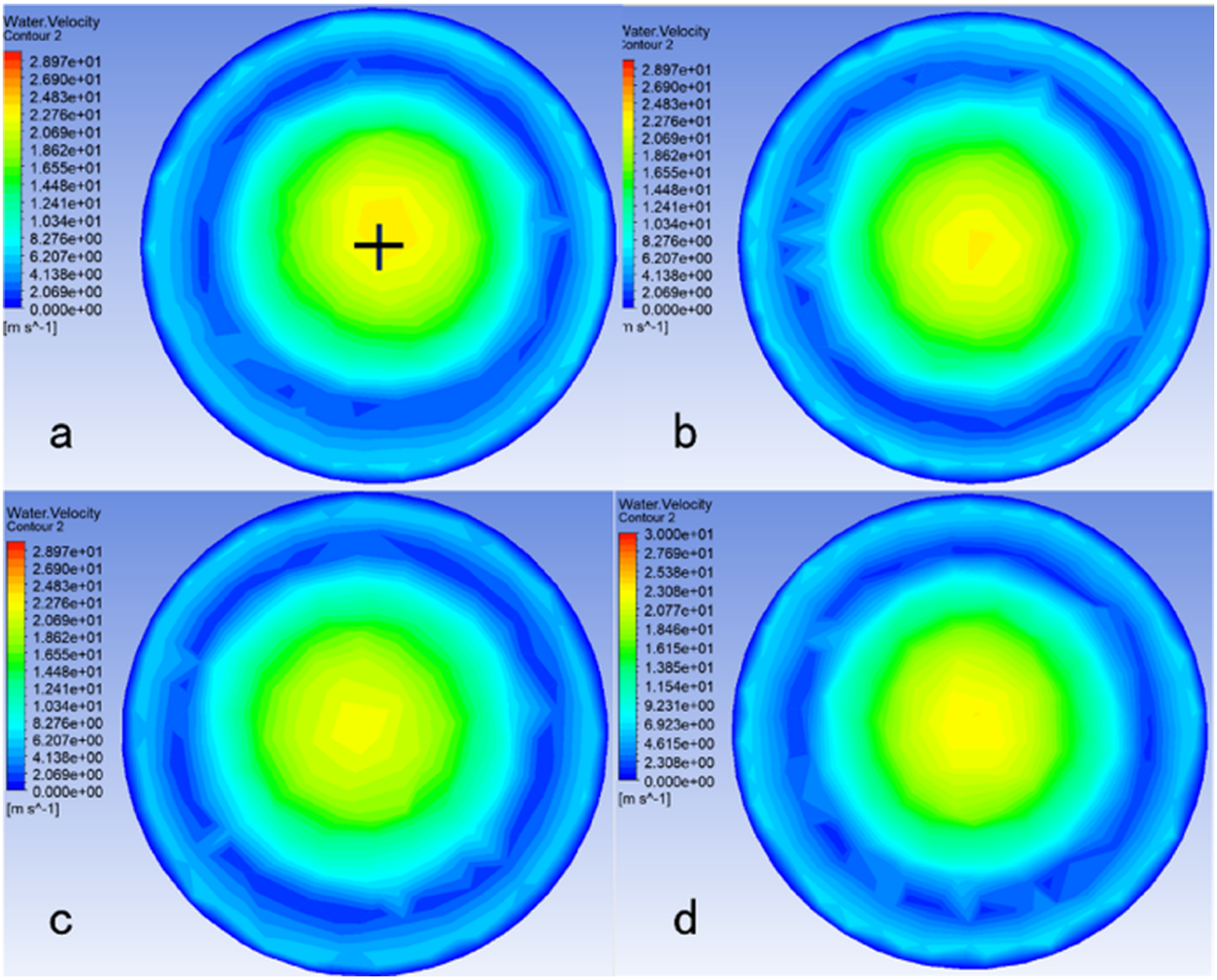

Figure 17. Cloud diagram of liquid phase velocity distribution with different length diameter ratios of the mixing cavity.

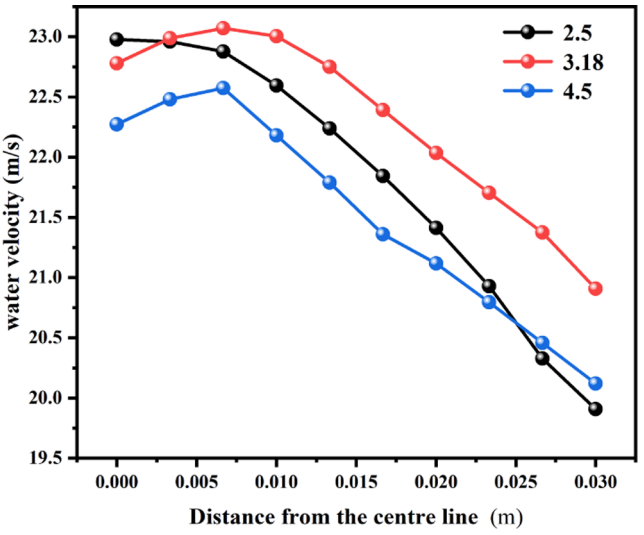

Figure 18. Liquid phase velocity distribution at different length diameter ratio sections of the mixing chamber.

foam and air flow field is uneven, resulting in a low jet range. At a higher liquid volume, the gas−liquid ratio is lower, and the gas−liquid ratio is 33 when the liquid volume is 18 m^3/h. While increasing the probability of gas−liquid collisions, there is less compressed air available for the unit foam mixture, and the mixing effect between the compressed air and the foam mixture is poor, resulting in a lower FER. The low-foam stream has a higher concentration, less friction with the air, and is not easy to diverge, thereby retaining a large amount of kinetic energy and being able to get a longer distance.

Table 6. Mean−Variance Table of Length Diameter Ratio of the Mixing Cavity

length diameter ratio sections of mixing chamber	average value	variance
2.5	21.80693	1.26425
3.18	22.29985	0.5806
4.5	21.51398	0.7676

It can also be seen from Figure 4 below that the foaming performance of the foam generator tends to increase in the 8−12.4 m^3/h range. In the 8−12.4 m^3/h range, the FER and half-life are negatively correlated, and the foaming effect cannot be improved by continuing to adjust the liquid volume. Therefore, at a fixed gas flow, the best foaming performance is achieved with a liquid volume of 12.4 m^3/h for gas−liquid coaxial jet foam generator.

https://doi.org/10.1021/acsomega.4c01862
ACS Omega 2024, 9, 31646−31656

4.2. Effect of Gas Flow Rate on Foaming Performance. According to the previous analysis, the best foaming performance is achieved at a fixed gas flow rate of 12.4 m^3/h in the foam generator. To investigate the effect of gas flow variation on foaming performance, the gas volumes were adjusted to 267.0, 356.9, 415.4, 526.0, and 597.9 m^3/h at a liquid flow rate of 12.4 m^3/h. Figures 5 and 6 below show the gas−liquid coaxial jet foaming performance changes with the gas volume when the liquid volume is 18 and 12.4 m^3/h respectively, corresponding to the above gas volume.

Figure 7 shows the variation of foam production performance with gas volume for a liquid volume of 8 m^3/h. The foaming range rises with increasing gas volume and then remains stable, while the rest of the foaming properties tend to rise and then fall with liquid volume, peaking at a gas volume of 356.9 m^3/h. At this point the FER is 40, the pressure air utilization rate is 0.9, the foam volume is 320 m^3/h, the half-life is 15 min, and the maximum range of 8 m is achieved at an air volume of 526.0 m^3/h. This is because the foaming agent foams with the gas due to the impact of the excess compressed gas and the foam has difficulty existing, producing an atomization phenomenon. Such phenomena were also found by Chen when studying foam generators for submersible drilling rigs.[11,26]

A comprehensive analysis of Figures 5−77shows that the foaming performance does not vary consistently with the gas volume in different intervals of the liquid volume value. When the liquid volume is higher than 12.4 m^3/h, increasing the air supply volume as much as possible will help to improve the foaming performance. When the liquid volume is below 12.4 m^3/h, the air volume cannot be increased, otherwise the foaming performance will be affected. It is necessary to find the best working conditions to optimize the foaming performance of the foam generator.

4.3. Effect of Outlet Diameters on Foaming Performance. The foam production performance of gas−liquid coaxial jet foam generator (numbered D1, D2, D3) with outlet diameters of 65 mm, 110 mm, and 220 mm was studied. Figure 8 shows the variation of FER with liquid volume under different outlet diameters. The data shows that the FER of D1 and D2 initially increases and then decreases with an increase in the gas−liquid ratio, with both reaching a peak. The maximum FER of D1 is 35 when the liquid volume is 10 m^3/h, and the maximum FER of D2 is 45 when the liquid volume is 12.4 m^3/h. For the same gas−liquid ratio, the FER of D2 is greater than that of D1. However, compared to the D3 FER, the overall FER of D1 and D2 are lower. At a liquid volume of 10 m^3/h, the D1 FER is 40% lower than that of D3. According to Bernoulli's theorem, the kinetic, potential, and pressure potential energies per unit volume of fluid in any section of the same flow tube remain constant under ideal conditions, due to the fact that the tapering structure bundles the foam in the foaming chamber, and the pressure energy of the foam is partly converted into kinetic energy of the foam. This makes it necessary for the liquid film to provide greater tension to counteract the diffusion of the gas, facilitating the defoaming process. At the same time, the foam collides, squeezes, and merges through the D1 exit diameter, which facilitates foam breakup and precipitation, thus reducing the FER.

Figure 9 shows the variation of half-life with liquid volume for different outlet diameters. The half-life of D1 and D2 foam increases and then decreases as the liquid volume increases. The maximum half-life is reached at a liquid volume of 10 and 12.4 m^3/h with a foam half-life of 11 and 15 min, respectively. The reason for the low half-life of D1 foam may be that the smaller outlet diameter increases the exit velocity of the foam streamer and intensifies the shear-breaking effect of the foam streamer against the pipe wall. This results in partial foam rupture and reduced foam uniformity, which, in turn, leads to reduced foam stability.

The half-life of D3 foam gradually decreases with increasing liquid content. Due to the thermodynamic instability of the foam, there is a decay process of the foam, in which there are three basic phenomena: liquid film discharge, bubble annexation, and bubble coarsening.[27−29] Combined with Figure 8 above, it can be found that with the increase of liquid volume, the FER decreases, and the thickness of the liquid film becomes thinner. Due to the drainage of the foam dominates, a large amount of foam liquid is precipitated, resulting in a lower half-life of the foam. When D1 and D2 are in the optimal liquid volume, the foam half-life is higher. This is because the FER of the foam increases and the thickness of the foam becomes thinner. When the foam drainage reduces to a certain thickness, according to the DLVO theory,[30] the separation pressure of the liquid film will prevent the further reduction of the thickness of the liquid film so that the liquid film drainage process reaches equilibrium. During this process, less liquid is released from the foam, thereby increasing the half-life of the foam. This phenomenon can be explained by Stevenson's two-phase foam system drainage velocity equation,[31] as shown in the following formula 3. The FER increases, d_{32} increases, μ decreases, and the foam half-life increases.

$$J_d = \frac{\rho_l g d_{32}^2}{\mu} m \varepsilon_l^n \tag{5}$$

where ρ_l is the density of the liquid, g/cm^3; g is the acceleration of gravity, m/s^2; d_{32} is the average diameter of the solitaire of the bubble, mm; ε_l is the liquid content of the foam, %; m and n are fitting parameters whose magnitude is mainly related to the type and concentration of the surfactant; and μ is the velocity of the liquid perpendicular to the Plateau boundary.

Reducing the outlet diameter and increasing the outlet kinetic energy have an impact on the stability of the foam. The foam half-life of D3 is higher than that of D1 as a whole, while D2 is longer than D3 when the liquid volume is 10−12.4 m^3/h. It shows that at this time, the high efficiency utilization of the cavity makes the foam mixture fully foam and the prepared foam is uniform. At the same time, the extrusion and rupture of the foam by the tapered outlet are relatively small, the prepared foam is uniform, and the half-life of the foam is improved.

Figure 10 shows the variation curve of the jet range with the gas-to-liquid ratio for different outlet diameters. The range of D2 and D3 increases as the gas−liquid ratio increases. It is evident that an increase in the gas−liquid ratio results in the complete foaming of the foam liquid, leading to a complete foam section in the foaming chamber. Under the action of continuous wind pressure, the foam is pushed and accelerated, which increases the exit kinetic energy of the foam, which is manifested as the increase of the foam jet range.

The range of D1 decreases and then increases with the increase of gas−liquid ratio, and the highest range is 24 m at the liquid volume of 18 m^3/h. Combined with Figure 6 above, it can be found that the changing trend of D1 FER is just opposite to the range. This is due to the fact that at gas volumes of 8 and 18 m^3/h, the FER is 20, the foam column is

https://doi.org/10.1021/acsomega.4c01862
ACS Omega 2024, 9, 31646−31656

dense, and the greater the gas−liquid ratio, the greater the power provided the longer the range of the foam column. In contrast, at an air volume of 10 m^3/h, the FER is high, and the foam streamer is gradually dispersed and shed by the continuous influence of air resistance after it has entered the air. Further increasing the friction area with the air reduces the range of the foam.

Confined spaces are characterized by a high degree of confinement, limited width and number of exits, and relative concealment, giving them specific characteristics that result in unique fire hazards. For example, confined space fires often result in severe oxygen depletion, rapid temperature rise, difficult smoke removal, slow heat dissipation, and difficult rescue situations. This requires that the flow rate of foam preparation is large enough to continuously pour foam into confined spaces and the use of the cooling and suffocation effects of foam to rapidly cool and eliminate the high-temperature fire area. For this reason, this paper compared the variation of foam volume with the gas−liquid ratio under different outlet structures. Figure 11 shows the variation of foam volume with liquid volume under different outlet diameters. It can be concluded that with the increase of the gas−liquid ratio, D3 first increases and then decreases, and it reaches the maximum value when the liquid volume is 10 m^3/h, and the foam volume is 580 m^3/h. D2 also exhibits the same pattern. When the gas−liquid ratio is 48, the maximum value is obtained, and the foam volume is 558 m^3/h, which is slightly lower than that of D3. The amount of foam in D1 is lower than the former two, and the overall value is below 360 m^3/h, which is not conducive to the generation of large-flow foam.

Figure 12 shows the variation of compressed air utilization rate with gas−liquid ratio under different outlet diameters. It can be seen that the φ of D2 and D3 both showed a trend of rising first and then decreasing, and the highest compressed air utilization rates were 97% and 93%, respectively. The φ of D1 is generally low, below 60%, which means that more compressed air is lost to the air than is used to produce foam.

4.4. Comparison of Foam Production Performance of Different Foam Generator. The foaming generator is one of the keys to the foaming effect of the foam mixture, and the foaming effect produced by different foam generators is also inconsistent. Table 2 is the experimental data table of the gas−liquid coaxial foam generator, Table 3 is the experimental data table of the Venturi foam generator, and Table 4 is the experimental data of spiral jet-type foam generator. It can be found that the gas−liquid coaxial jet foam generator, at the gas−liquid ratio of 48, has a FER 45 times higher than the venturi foam generator (30 times), the range of 10 m is also higher than the venturi foam generator 5 m, the amount of foam generated is also 50% higher than the venturi foam generator. Figure 13 shows the foaming effect of gas−liquid coaxial and venturi tube foam generator, and the above point can be further validated.

4.5. Influence of Structural Dimensions on Gas−Liquid Coaxial Jet Foam Generator. A simulation of a coaxial gas−liquid foam generator with different configurations has been carried out for the analysis of the distribution of the internal flow field, which cannot be observed inside the foam generator. The size and uniformity of the liquid phase velocity directly determine the mixing effect of the gas−liquid two-phase and the kinetic energy of the foam outlet. This has a significant impact on the foam production performance of the foam generator.

4.5.1. Gas−Liquid Coaxial Jet Foam Generator Geometry Model. The model of the gas−liquid coaxial jet foam generator has been described in the previous section. The wall thickness of the whole model is 2.5 mm. Table 5 displays the quality of the mesh created using fluent meshing, as illustrated in Figure 14, and the quality of the mesh meets the computational requirements.

4.5.2. Fluent Key Parameter Settings. 4.5.2.1. Physical Properties of Gas and Liquid Phases. Air and liquid water was selected as the fluid flow medium, where the density of liquid water: 998.2 kg/m^3, viscosity: 0.001003 kg·$m^{-1}s^{-1}$, the density of air: 1.225 kg/m^3, viscosity: 1.7894 × 10^{-5} kg·$m^{-1}s^{-1}$, and gravity: −9.81m/s^2.

4.5.2.2. Model Setup. The simulation model selected is the mixture model because the device works within the gas phase and liquid phase flow, and interphase mixing occurs. The gas phase inlet velocity was set to 83 m/s, liquid phase inlet was set to 2.67 m/s, and the calculation of the Reynolds numbers of 127 585 and 284 103, respectively, are turbulent flow, so we adopted the turbulence model of the Realizable k-ε model. The boundary conditions of the gas−liquid phase inlet are defined by the intensity and hydraulic diameter parameters. The boundary conditions at the gas−liquid phase inlet were set to intensity and hydraulic diameter.

4.5.2.3. Boundary Conditions. The gas phase inlet was set as the velocity inlet, and the liquid phase inlet was set as the pressure inlet, with the inlet pressure of 0.8 MPa and the outlet pressure of 0.1 MPa. The wall conditions of the model were set to be adiabatic, static, and no-slip wall boundaries, and a standard roughness model was used.

4.5.2.4. Turbulence Intensity Calculation. Because of the turbulent flow inside the model, it is necessary to define the inlet turbulent kinetic energy k and turbulent kinetic energy dissipation rate ε. These parameters are typically defined in one of four ways: by providing initial values for k and ε, by specifying turbulence intensity and turbulence length, by providing the ratio of turbulence intensity to turbulence viscosity, or by specifying turbulence intensity and hydrodynamic diameter. This paper used the fourth method of definition to determine turbulence intensity and hydrodynamic diameter. The remaining parameter values are calculated using the following formula

$$I \approx 0.16\mathrm{Re}^{-1/8} \tag{6}$$

$$k = \frac{3}{2}(I\bar{u})^2 \tag{7}$$

$$\varepsilon = C_u^{3/4}\frac{k^{2/3}}{l} \tag{8}$$

$$l = 0.07L \tag{9}$$

where I is the turbulence intensity, u is the average speed of the inlet, u is the average speed of the inlet, L is the characteristic length, Re is the Reynolds number, C_u is the empirical constants for turbulent fluids (0.09).

The gas−liquid phase turbulence intensity at the inlet of the coaxial jet mesh foam generator was calculated to be 5.08%.

4.5.2.5. Solving. After initialization, set the step size for the simulation and observe whether the simulation converges through the residual Figure 15; generally, the residual less than 10^{-4} can be considered to converge. Figure 16 shows the internal flow field of the foam generator after convergent.

https://doi.org/10.1021/acsomega.4c01862
ACS Omega 2024, 9, 31646−31656

4.5.3. Simulation Results of Foam Generator Structure. As a mixing space for gas and liquid phases, the structural parameters of the mixing chamber directly affect the mixing effect. In this paper, the influence of the mixing chamber on the liquid phase velocity and uniformity is investigated by changing the structural parameter of the mixing chamber length diameter ratio (the ratio of the length to the maximum diameter). Four different length diameter ratios of 2.0, 2.5, 3.18 (Used in the experiment), and 4.5 are set to study the effect on the flow state of the internal flow field. The cross-sectional cloud diagram is shown in Figure 18.

In Figure 17, a, b, c, and d are the cases at length diameter ratios of 2.0, 2.5, 3.18, and 4.5, respectively. The center of the gas−liquid two-phase mixing jet in the cloud diagram of the group has a large deviation from the axis of the mixing chamber of the device, which affects the foaming of the device. Since the cross-sectional cloud diagram cannot quantitatively express the remaining three different cases, a 0.03 m long line segment is drawn from the axis and the three cases b, c, and d are quantitatively analyzed according to the velocity changes on the line segment. The velocity change curve of the liquid phase is shown in Figure 18.

Table 6 presents the mean and variance of the three mixing chamber length diameter ratios. It is clear that the liquid phase velocity is superior in both mean and variance compared to the other two when the length diameter ratio is 3.18. Therefore, the length diameter ratio of 3.18 is selected as the optimal mixing chamber length diameter ratio. However, there is no significant difference among the mean values of the three groups. Considering the foaming effect achieved by the previous test group, it is also possible to create foam at mixing chamber length diameter ratios of 2.5 and 4.5. However, their effects may be slightly inferior to that of the length diameter ratio of 3.18.

5. CONCLUSIONS

In view of the fact that there is no gas−liquid mixer with high efficiency and low resistance foaming for CAFS, a gas−liquid coaxial jet foam generator is designed for CAFS to prepare foam. The optimal working parameters of the foam generator are determined through experiments, and the influence of liquid flow rate, gas flow rate, and outlet diameter on FER, foam half-life, and shooting range are analyzed. The foam production effect of similar foam generator was compared. The main conclusions are as follows:

(1) When the liquid volume is in the range of 8−12.4 m^3/h, the foaming performance of the foam generator is on the rise. At this time, the optimum working condition of foam production has not yet been reached. When the liquid volume is in the range of 8−12.4 m^3/h, the FER and half-life are negatively related to it, and the foaming effect cannot be improved by continuing to adjust the liquid volume. Therefore, under a fixed gas flow rate, when the liquid volume of the foam generator is 12.4 m^3/h, the foaming performance is the best.

(2) It can be found that the liquid volume value is in different ranges, and the foaming performance varies with the air supply volume. If the liquid volume is higher than 12.4 m^3/h, increasing the air supply volume as much as possible will help to improve the foaming performance. However, when the liquid volume is lower than 12.4 m^3/h, the air volume cannot be increased blindly, and the best working conditions need to be sought to optimize the foaming performance of the foam generator.

(3) When the diameter of the foaming chamber is larger than that of the outlet structure, the effect of the gas−liquid ratio on the FER is not monotonous, and there is an optimal value. D2 has the best FER of 45 when the liquid volume is 12.4 m^3/h. While reducing the outlet diameter and increasing the outlet kinetic energy, it also affected the stability of the foam. The overall half-life of D3 foam was higher than that of D1, while D2 was greater than D3 when the liquid volume was 10−12.4 m^3/h.

(4) The gas−liquid coaxial jet foam generator has better advantages compared with similar devices in terms of FER and range and has better application prospects for fire control in restricted spaces. The foaming effect of a gas−liquid coaxial foam generator with different structures was explored with the help of fluent simulation. In terms of gas−liquid velocity distribution, the device has better size adaptability.

AUTHOR INFORMATION

Corresponding Author

Xiaoxing Zhong − *Key Laboratory of Gas and Fire Control for Coal Mines, Ministry of Education, China University of Mining and Technology, Xuzhou 221116, China; School of Safety Engineering, China University of Mining and Technology, Xuzhou 221006, China;* orcid.org/0000-0003-4477-780X; Email: zhxxcumt@cumt.edu.cn

Authors

Caiyuan Lu − *Key Laboratory of Gas and Fire Control for Coal Mines, Ministry of Education, China University of Mining and Technology, Xuzhou 221116, China; School of Safety Engineering, China University of Mining and Technology, Xuzhou 221006, China;* orcid.org/0009-0002-0685-2629

Mujun Chen − *Key Laboratory of Gas and Fire Control for Coal Mines, Ministry of Education, China University of Mining and Technology, Xuzhou 221116, China; School of Safety Engineering, China University of Mining and Technology, Xuzhou 221006, China*

Yuntao Liang − *Key Laboratory of Gas and Fire Control for Coal Mines, Ministry of Education, China University of Mining and Technology, Xuzhou 221116, China; School of Safety Engineering, China University of Mining and Technology, Xuzhou 221006, China; State Key Laboratory of Coal Mine Safety Technology, China Coal Technology & Engineering Group Shenyang Research Institute, Shenfu Demonstration Zone, Fushun 113122, China*

Complete contact information is available at: https://pubs.acs.org/10.1021/acsomega.4c01862

Notes

The authors declare no competing financial interest.

ACKNOWLEDGMENTS

This work was supported by the Key Program of the National Natural Science Foundation of China (grant no. 52130411) and the National Natural Science Foundation of China (grant no. 52074286).

https://doi.org/10.1021/acsomega.4c01862
ACS Omega 2024, 9, 31646−31656

REFERENCES

(1) Yang, G. The Analysis of the Development and Application Status of Compressed Air Foam Fire Extinguishing Systems. In *Proceedings of the 2011 Annual Academic Conference of the China Occupational Safety and Health Association: China Coal Industry Publishing House, 2011*, pp 383−387.

(2) Record high fire response in 2021 with 745,000 fires put out. [EB/OL]. https://www.119.gov.cngksjtj202226442.shtml.

(3) Yueyong, W.; Zhen, Y.; et al. Experimental study on the burn resistance of compressed air foam fire fighting. *Fire Sci. Technol.* **2022**, *41* (11), 1542−1546.

(4) Na, L.; Xing, Z.; et al. Review of research on the application of compressed air foam systems for fire protection of large storage tanks. *J. Wuhan Univ. Technol.* **2018**, *40* (03), 265−270.

(5) Jiaqing, Z.; Yong, H. et al. A Mixing Device for Compressed Air Foam Fire Extinguishing Systems. CN113577609A2021.

(6) Jia, L.; Jiang, B. et al. Gas-Liquid Mixing Units and Fire Engines. CN213433889U2021.

(7) Jie, L.; Zhijiong, H. et al. Compressed Air Foam Fluid Mixing Units. CN212700173U2021.

(8) Cheng, H.; Zhiming, B. et al. A Compressed Air Foam Gas-liquid Mixer and Design Method. CN112156403A2021.

(9) Ye, Y. *Study of Gas-liquid Mixing Characteristics of Compressed Air Foam Systems and Experimental Setup*; Huazhong University of Science and Technology, 2019.

(10) Xinixao, L. *Research on Efficient Preparation Technology and Application of Foam to Prevent Spontaneous Combustion of Coal in Large Spaces*; China University of Mining and Technology, 2016.

(11) Jushi, C.; Zhongan, J.; et al. Experiments on foam generator and its flow characteristics during DTH drill in open-pit mine. *J. China Coal Society* **2015**, *40* (S1), 132−138.

(12) Chen, J. Property experiments on the foam generator and its influencing factors during down-the-hole drilling. *Process Saf. Environ. Prot.* **2018**, *114*, 169−178.

(13) Lei, P.; Wenmin, H.; et al. Research on the composite foam generator and its foaming properties for earth pressure balance shiel. *J. Railway Sci. Eng.* **2020**, *17* (12), 3199−3207.

(14) Youying, M.; Mengyao, X.; et al. Experimental study on the influence of structural parameters on foaming performance of mesh foaming machine for mine. *Ind. Safety Environ. Protection* **2019**, *45* (05), 92−95.

(15) Qin, B.; Wang, D.; et al. Foaming mechanism and design principles of a three-phase-foam generator. *J. China Univ. Mining Technol.* **2008**, *04*, 439−442.

(16) Minwen, S.; Xiaoqiang, D. et al. Concentric tube foam generator [P]. CN105275445B2010.

(17) Stec, M.; Synowiec, P. M. Study of fluid dynamic conditions in the selected static mixers part III-research of mixture homogeneity. *Can. J. Chem. Eng.* **2018**, *97*, 995−1007.

(18) Brian, H.; Zhang, B.; et al. Improved research-scale foam generator design and performance characterization. *J. Loss Prev. Process Ind.* **2016**, *39*, 173−180.

(19) Fu, G.; Jiang, J.; Ni, L. Research-scale three-phase jet foam generator design and foaming condition optimization based on Box−Behnken design. *Process Saf. Environ. Prot. 134*, 217 225.

(20) Yang, J.; Li, Y.; Zhu, J.; et al. Quantitative study of the factors of LNG liquid foam stability Operating parameters and collection containers and time. *Process Saf. Environ. Prot.* **2018**, *117*, 223−231.

(21) Liu, C.; Zhang, W.; et al. Design and internal flow characteristics of a spiral baffle type foam generator. *J. Math. Pract. Theory* **2018**, *48* (08), 120−127.

(22) Liu, C.; Liu, G.; et al. Experimental study of the effect of gas phase pressure on a baffle-type foam generator. *Contemporary Chem.* **2019**, *48* (01), 144−146.

(23) Hewei, L.; et al. Research Status of Gas-Liquid Mixer in Compressed Air Foam Fire Extinguishing System. *Mech. Res. Appl.* **2021**, *34* (06), 203−206.

(24) Sheng, Y.; Lu, S.; et al. Drainage of aqueous film-forming foam stabilized by different foam stabilizers[J]. *J. Dispersion Sci. Technol.* **2018**, *39*, 1266 DOI: 10.1080/01932691.2017.1393432.

(25) (a) Song, X.; Cui, X.; et al. Multi-parameter screening study on the static properties of nanoparticle-stabilized CO2 foam near the CO2 critical point. *Arabian J. Chem.* **2022**, *15*, 103676.

(26) Experiments on properties of foaming generator during down-the-hole drilling in open-pit mine[J]. *J. Harbin Inst. Technol.* **2016**, *484* 166 171.

(27) Farhadi, H.; Riahi, S.; Ayatollahi, S.; et al. Experimental study of nanoparticle-surfactant-stabilized CO2 foam: Stability and mobility control. *Chem. Eng. Res. Des.* **2016**, *111*, 449−460.

(28) Qin, B.; Lu, Y.; Lib, Y.; et al. Aqueous three-phase foam supported by fly ash for coal spontaneous combustion prevention and control[J]. *Adv. Powder Technol.* **2014**, 1527−1533.

(29) Yekeen, N.; Kamal Idris, A.; A, M.; Samin, A. M.; Risal, A. R.; Kun, T. X.; Manan, M. A. Bulk and bubble-scale experimental studies of influence of nanoparticleson foam stability. *Chin. J. Chem. Eng.* **2017**, *25*, 347−357.

(30) Liu, Z.; Bode, V.; Hadayati, P.; et al. Understanding the stability mechanism of silica nanoparticles: The effect of cations and EOR chemicals. *Fuel* **2020**, *280*, No. 118650.

(31) Ireland, P. M.; Jameson, G. J. Liquid transport in a multi-layer froth[J]. *J. Colloid Interface Sci.* **2007**, No. 314, 207−213.

https://doi.org/10.1021/acsomega.4c01862
ACS Omega 2024, 9, 31646−31656